INDIAN JOURNAL OF SCIENCE AND TECHNOLOGY

RESEARCH ARTICLE

Study of Conduction Mechanisms in Alkali and Transition Metal Oxides Doped Borosilicate Glasses

Aravind Dyama[1], T Sankarappa[1]*, Mohansingh Heerasingh[1], Ashwini Devidas[1], Pallavi Jamadar[1], Amarkumar Malge[1]

1 Department of Physics, Gulbarga University, Kalaburagi, 585106, Karnataka, India

OPEN ACCESS

Received: 14-02-2024

Accepted: 27-03-2024

Published: 23-04-2024

Citation: Dyama A, Sankarappa T, Heerasingh M, Devidas A, Jamadar P, Malge A (2024) Study of Conduction Mechanisms in Alkali and Transition Metal Oxides Doped Borosilicate Glasses. Indian Journal of Science and Technology 17(17): 1767-1775. https://doi.org/10.17485/IJST/v17i17.412

* **Corresponding author**.

sankarappa@rediffmail.com

Funding: None

Competing Interests: None

Published By Indian Society for Education and Environment (iSee)

ISSN
Print: 0974-6846
Electronic: 0974-5645

Abstract

Objectives: To synthesise a unique set of borosilicate glasses of composition, $xLi_2O + 0.15SiO_2 + 0.45B_2O_3 + 0.05ZnO + (0.35 - x)\ WO_3$; ($0.25 \leq x \leq 0.34$) and to investigate conduction mechanisms. **Methods**: Glasses were synthesized by melt quenching technique. From the XRD spectra samples were conformed to be non-crystalline in nature. Density has been measured by following Archimedes principle and is found to decrease with Li_2O mole fractions in the range 2.900 gm/cm^3 – 2.495 gm/cm^3. DC-conductivity was measured for the temperature range 303K – 525 K using two probe technique. **Findings:** It was found that these glasses behave like semiconductors in terms conductivity variation with temperature. Conductivity decreased with Li_2O content up to 0.33 mole fractions and increases for higher mole fractions. High temperature conductivity variation i.e., above $\Theta_D/2$ (Θ_D = Debye's temperature) is found to follow the Mott's small polaron hopping (SPH) model. Activation energy for conduction above $\Theta_D/2$ is found to be in the range 0.282 eV-0.702 eV. Decrease of conductivity and activation energy with increase of Li_2O content has been explained in terms of dynamic nature of network and formation of cation-polaron neutral entities. The conductivity below $\Theta_D/2$ has been found to follow Mott's variable range hopping (VRH) models. The density of states at Fermi level derived from Mott's VRH are found to be of the order of 10^{23} eV^{-1}cm^{-3} which are in close agreement with reported ranges for transition metal oxides doped glasses. **Novelty**: A unique set of mixed conducting borosilicate glasses have been prepared and investigated thoroughly for conduction mechanisms.

Keywords: Borosilicate glasses; Density; Conductivity; Activation energy; Density of states

1 Introduction

Glasses are the oldest materials known to us. They vary in composition, homogeneity, and versatility for diverse applications. Borosilicate glasses, combining B_2O_3 and SiO_2, feature low thermal expansion, high softening temperature and mechanical strength useful for photovoltaic cells and displays. Doping borosilicate glasses with alkali oxides such as Li_2O improves network compactness and provides moisture resistance.

Transition metal ions in glasses induce conductivity which is crucial for high energy density solid-state batteries [1–4].

ZnO when present in lower proportions in the glasses, it serves as a dynamic network modifier. It also reduces melt viscosity and actively reinforces network integrity while regulating crystallization dynamics [5]. The incorporation of tungsten oxide, WO_3 in borosilicate glasses enhances conductivity and dielectric characteristics significantly. Tungsten ions influence glasses' physical properties because of their existence in different valence states such as W^{4+}, W^{5+} and W^{6+}. The electron hopping between the ions of different valence states i.e., lower to higher valence states produces electrical. This feature makes 3d-transition metal ion-doped glasses very interesting due to their unique electrical and spectroscopic properties [6,7].

The mixed electronic-ionic conducting glasses have become very important in scientific and technological fields due to their potential applications in solid state batteries, cathode materials, optoelectronic devices etc. Electronic conduction in these glasses arises due to the presence of transition metal oxide content and ionic conductivity is because of alkali ion concentration. Incorporation of transition metal oxides such V_2O_5, Fe_2O_3, MnO, WO_3 etc into glass network produces semiconduction and alkali oxides such as Na_2O, Li_2O, K_2O etc produces ionic conduction. The simultaneous presence of TMO and alkali oxides in glasses makes electronic and ionic conductions compete with each. The predominance of each of these conductions prevails in different compositional domains of the glasses. The network modifiers such as alkali oxides reduce melting temperature of the glasses and influences electrical properties [1]. In borosilicate glasses, alkali oxides tend to convert three coordinated boron $[BO_3]$ trigonal units into four coordinated boron $[BO_4]^-$ tetrahedral units. In the case of borate glasses, it was hinted that if Li_2O content exceeds 25%, non-bridging oxygens (NBO) can be achieved [8] leading to decrease in glass network connectivity. In either case, mobile ions are produced and allowed to move which affects ionic conductivity.

The influence of alkali and alkaline earth oxides on borosilicate glasses has been investigated and found that there exist optimum compositions of the glass for which excellent thermal properties and coefficient of thermal expansion (CTE) can be achieved [9]. CTE depends on the strength of Si-O bonds which can be varied with alkali content. Recent studies have investigated the impact of different transition metal oxides on the formation, thermal, electrical etc properties of TiO_2-borosilicate glasses and glass ceramics. The findings revealed that they greatly enhance electrical conductivity and ZnO in particular has notable impact on conductivity [10]. AC conductivity through dielectric properties has been probed thoroughly for V_2O_5 and WO_3 doped lithium borosilicate glasses [7]. It was reported that ac conductivity increased with increase of WO_3 content up to 8 mol % and then decreased for further amounts of WO_3. Activation energy behaved opposite to that of WO_3 content. Optical band gap behaved exactly the similar way as that of activation energy for conduction. However, it is to be noted that in these studies, the effect increase of WO_3 at the cost of V_2O_5 has been the main focus. Dielectric studies were reported for zinc-boro-tellurite glasses containing Li_2O and WO_3 but the data analysis was not extended up to ac conductivity [5].

The aim of this study is to investigate influence of alkali and transition metal oxides on the structure, physical and electrical properties of borosilicate glasses; $Li_2O \bullet SiO_2 \bullet B_2O_3 \bullet ZnO \bullet WO_3$. This offers a unique opportunity to understand conduction mechanisms in borosilicate glasses having both alkali and transition metal oxides. We tried to analyze the conductivity variation with increase of transition metal oxide (polaron producer) content at the expense of alkali oxide (ions producer) content. That makes these glasses special and unique. We determined the activation energy for dc conduction, Debye's temperature, and density of states at Fermi level that throw light on fundamental properties of the glasses. There are no research articles offering data on the glasses of the present composition.

2 Methodology

The glasses in the composition batch of x Li_2O + 0.15 SiO_2 + 0.45B_2O_3 + 0.05ZnO + (0.35 – x)WO_3; x = 0.25, 0.26, 0.28, 0.30, 0.33, 0.34, were prepared by standard melt-quenching technique and labelled as BSZWL1, BSZWL2, BSZWL3, BSZWL4, BSZWL5 and BSZWL6 respectively. The AR grade chemicals from Himedia, Lithium carbonate (Li_2CO_3), Silicon dioxide (SiO_2), Boric acid (H_3BO_3), zinc oxide (ZnO), and Tunstic acid (H_2WO_4) were used as starting materials. The appropriate mole fractions of individual chemicals were weighed, mixed and taken in silica crucibles. It was melted in a muffle furnace at 1273K. The melt was quenched to room temperature between two stainless steel plates. The samples were annealed at 450K for 24 hours. Powdered samples were subjected to XRD and their phases were confirmed. XRD experiments were carried out in a Rigaku make diffractometer with Cu-Kα radiation in the Bragg's angle range 10^0-80^0.

Density, D of the samples was measured using Vibra (Essae) make HT – series analytical balance by applying Archimedes principle. According to this, the buoyancy equals the weight of the displaced fluid. Xylene (= 0.865 g/cm^3) was used as an immersion liquid. Density was estimated using the expression [11],

$D = \frac{W}{W-W_L} X D_L$

Where, W is the weight of the sample in air, W_L weight of the sample in liquid and D_L the density of a buoyant liquid.

For dc conductivity measurement, the samples of thickness 3 to 4 mm and cross-sectional areas in the range 46 mm^2 - 61.5 mm^2 sizes were selected. Silver paint was applied on two major surfaces of the samples to form electrodes. The conductivity

measurements were done using two probe method in the temperature range 300 K–525 K. A fixed voltage (V) of 10V from a constant voltage source was applied across the sample and the current (I) flowing through was measured using a high precession pico ammeter. The temperature of the samples was measured using a Chromel (Cr)-Alumel(Al) thermocouple and micro volt meter. Resistance, R was determined as (V/I) and from which the resistivity, ρ was estimated as, $\rho = \frac{1}{R}\left(\frac{T}{A}\right)$ with A being cross-sectional area, and t the thickness of the glass sample. The conductivity was determined as $\sigma = (1/\rho)$ within error limit of 2 to 3 %.

Table 1. Formulae used to calculate physical parameters of BSZWL glasses

Parameter	Formula	Description
1. Molar Volume	$V_m = M_{AV}/D$	M_{AV} = average molecular weight
2. Density of TMIs	$N=2[\{\rho(m_{ZnO}+m_{WO_3})/(M_{ZnO}+M_{WO_3})\}N_A]$	m_{ZnO} & m_{WO_3} = mole fractions, M_{ZnO} & M_{WO_3} = Molecular weight, N_A = Avogadro's number
3. Small polaron radius	$r_p = 0.5(\pi/6N)^{1/3}$	N = Density of TMI
4. Mean Spacing between TMIs	$R = (1/N)^{1/3}$	

3 Results and Discussion

3.1 XRD

XRD pattern collected for the present samples are displayed in Figure 1. XRD pattern shows no sharp peaks which indicate amorphous nature of the samples. However small peak cantered at 42.46^0 is commonly observed for all samples. The crystallite sizes corresponding to this peak were determined using Debye-Scherrer's formulae to be varying from 0.063 nm to 0.079 nm. So, the present samples can be considered as glass-nanocomposites. The nano-crystallites were reported previously for alkali oxides doped zinc-boro-phosphate glasses[12].

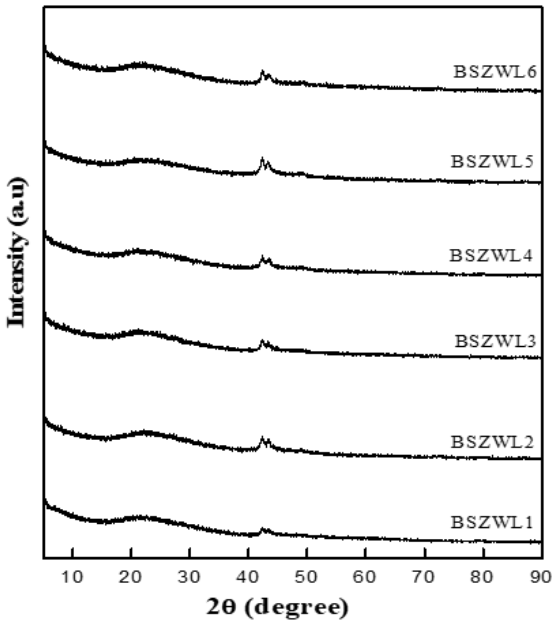

Fig 1. XRD patterns of BSZWL Glasses

3.2 Density and Molar volume

Density D of the present glasses is found in the range 2.900 gm/cm^3 - 2.495 gm/cm^3. Molar volume V_m obtained is in the range 38.680cm^3/mol- 44.569cm^3/mol. Density is found decreasing and molar volume increasing monotonously with increasing Li_2O content (Figure 2). This informs that network is going loose packed continuously with increase of mole fractions of Li_2O. Mean spacing between transition metal ions, R, transition metal ion density, N and small polaron radius r_p wereestimated using the expressions given in [13]. The N values are found increasing and R and r_p decreasing with increase of mole fractions of Li_2O (see Table 2). These density and molar volume values are comparable with reported values of lithium doped borosilicate glasses [14,15]. The decrease in r_p can be understood from the fact that the concentration of polaron hopping centres increases with increase in transition metal oxide concentration, N. The N, R and r_p values are comparable with Dy_2O_3-Li_2O-B_2O_3-SiO_2 glasses [13].

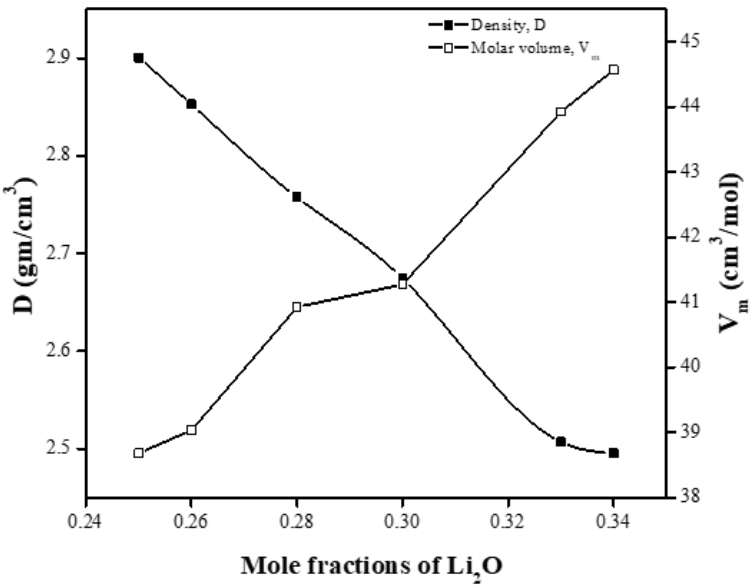

Fig 2. Variation of density (D) and molar volume (V_m) with mole fractions of Li_2 O

Table 2. Physical parameters of BSZWL glasses

Sample	Mole Fractions of Li_2O	Density, D (gm/cm^3) ± 0.005	Molar volume, Vm (cm^3/mole) ±0.004	Density of TMI, N x 1021 (cm-^{3})	Mean spacing between TMIs, R (nm)	Small polaron radius, rp (nm)
BSZWL 1	0.25	2.9003	38.68	7.7855	0.5045	0.4362
BSZWL 2	0.26	2.8526	39.037	7.0182	0.5223	0.4515
BSZWL 3	0.28	2.7572	40.924	8.7045	0.4861	0.4202
BSZWL 4	0.3	2.6744	41.2745	9.3481	0.4747	0.4104
BSZWL 5	0.33	2.5067	43.9258	10.156	0.4617	0.3992
BSZWL 6	0.34	2.4954	44.5691	12.01	0.4366	0.3775

3.3 DC Conductivity

The electrical conductivity is observed to increase with increasing temperature revealing semiconducting nature. The conductivity variations for the measured range of temperature are found to lie in the range from 10^{-4} to $10^{-5}(\Omega m)^{-1}$. The plots of conductivity, σ versus temperature, T, for all BSZWL glasses are shown in Figure 3. A close look at the conductivity variation reveals that most of the glasses had no measurable conductivity at least up to 400K and increases after that. That is why the

conductivity data for temperature above 400K has been subjected to further analysis.

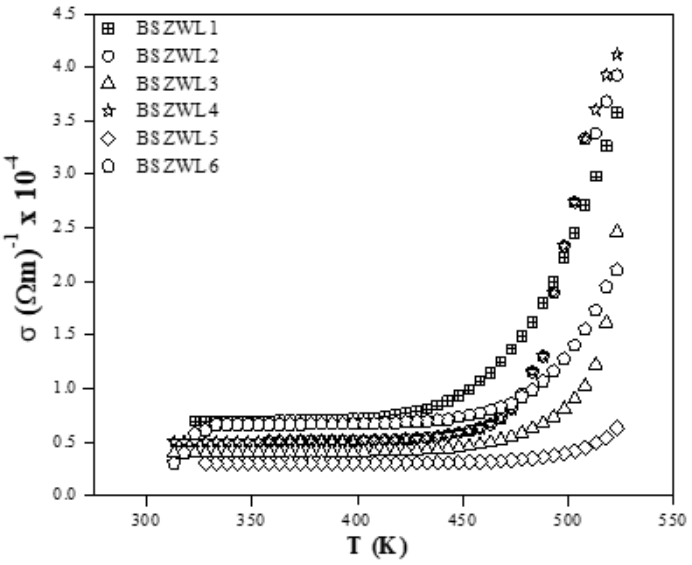

Fig 3. Conductivity (σ) versus temperature (T) of BSZWL glasses

Mott's small polaron hopping model has been applied to understand conductivity behaviour with temperature. According to this model, σ is expressed as[16],

$\sigma = (\sigma_o/T) \exp(-W/K_BT)$

Where, W is the activation energy and σ_o the pre-exponential factor.

The plots of $\ln(\sigma T)$ versus (1/T) for all the samples were drawn and shown in Figure 4. Linear lines were fit to the data. From the fits it can be observed that the fit lines are deviating from the data below certain temperature, T_D. This means that above T_D, SPH model is adequate to explain conductivity changes with temperature. Using T_D, Debye's temperature θ_D has been estimated as, $\theta_D=2T_D$ and recorded in Table 3. The θ_D increases with increase of Li_2O up to 0.30 mole fractions and decreases for higher mole fractions. From the slope of the fit liner lines, the activation energy for dc conduction, W for each sample has been determined. It is found to lie in the range 0.282 eV to 0.703 eV. These W values closely agree with Fe_2O_3 doped sodium-borosilicate glasses[3].

To understand the behavior of conductivity and activation energy with Li_2O content, Conductivity at 490K and activation energy, W are recorded in Table 3. It can be seen that conductivity and activation energy both decreasing in a zigzag form up to 0.30 mole fractions and increases later. It is known that the present glasses are mixed conducting type having both ionic and polaronic parts. The total conductivity at any temperature of interest can be expressed as, $\sigma_T = \sigma_i + \sigma_p$, where σ_i and σ_p represent ionic and polaronic contributions to total conductivity, σ_T. From Table 2, it is clear that transition metal ion densities, N increases and inter spacing between transition metal ions, R decreases with increase of Li_2O content. This means that polaronic contribution, σ_p can be expected to increase. At the same time ionic contribution, σ_i should also increase with increase of Li_2O content because more and more number of ions are added to the glass matrix. Therefore, σ_T must increase with Li_2O concentration. But data displayed in Table 3 indicates contrary to that. This behaviour of conductivity and activation energy can be attributed to the dynamic nature of structural variations in the glass network by way of producing bridging oxygens (BOs) and non-bridging oxygens (NBOs).

Another possible reason one can offer for the decrease of conductivity with increase of Li_2O content is that with increase of Li_2O content, there will be the production of some cation-small polaron neutral entities. This decreases ionic conductivity and hence over all conductivity. At the same time, the polaron hopping of the left out polarons may become easy hence decrease in their activation energy for conduction. Similar explanation was provided for simultaneous decrease of conductivity and activation energy[17]. Generally, in most glasses, conductivity and activation energy behaves opposite to one another[5,8]. A switch over conduction mechanisms from ionic to electronic, for a particular composition, has been observed in mixed

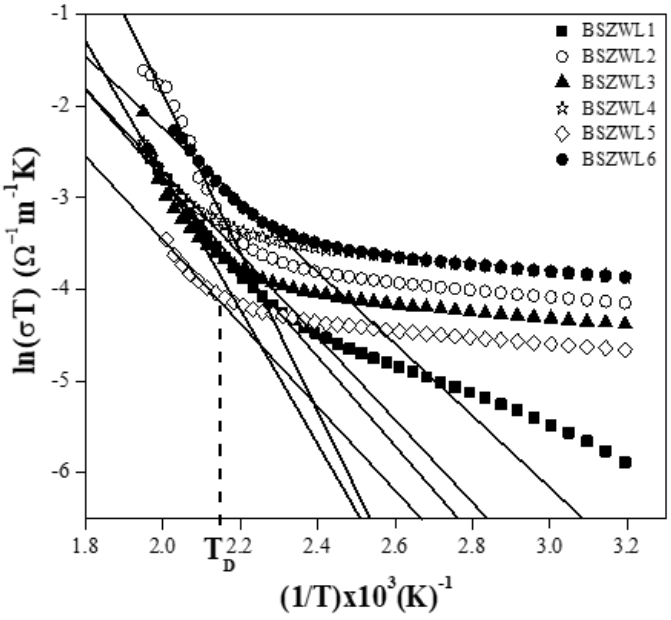

Fig 4. Plots of ln(σT) versus (1/T) for all BSZWL glasses

Table 3. Activation energy (W), conductivity (σ) at 490K and N(E_F) values obtained from VRH and GVRH model fits at low temperature

Sample	Activation Energy W (eV)	σ x 10^{-4} at 490K	T_D (K)	Θ_D (K)	Mott's VRH Model N(E_F) x 10^{23} $eV^{-1}cm^{-3}$	Greave's VRH Model N(E_F) x 10^{29} $eV^{-1}cm^{-3}$
BSZWL1	0.435	2.448	433	866	0.603	0.237
BSZWL2	0.664	2.735	463	926	0.307	0.243
BSZWL3	0.702	0.899	468	936	7.480	0.154
BSZWL4	0.336	1.104	473	946	1.245	0.292
BSZWL5	0.282	0.539	458	916	6.008	0.360
BSZWL6	0.330	2.105	443	886	8.418	0.358

conducting glasses[18]. No such transition is evident in the present glasses.

The changes in conductivity with temperature below T_D have been looked into in view of variable range hopping models due to Mott and Greaves. As per Mott's model, the conductivity is given by[16],

$\sigma = A \exp(-B/T^{-1/4})$

Where, $A = [e^2/2(8\pi)^{1/2}]\ \nu_0[N(E_F)/\alpha k_B T]^{1/2}$ and $B = 4[2\alpha^3/9\pi k_B N(E_F)]^{1/4}$

The Mott's VRH plots of ln(σ) versus ($T^{-1/4}$) are shown in Figure 5. The linear lines were fit as shown in the figure and constants A and B were extracted. Using constant B, the density states per unit volume at Fermi level, N(E_F)were determined by taking $\alpha = 2x10^{10}$.

Conductivity at low temperature as per Greave's VRH model is expressed as[16],

$(\sigma T^{1/2}) = A \exp(-B/T^{-1/4})$

Where, A and B are constant. The greave's VRH Plots of $\ln(\sigma T^{1/2})$ versus ($T^{-1/4}$) are shown in Figure 6. The linear lines were fit the data and constants A, B were determined. Using the value of B, N(E_F) was determined using the equation,

$B = 2.1\left[\frac{\alpha 3}{k_B N(E_F)}\right]$

N(E_F) obtained from both Mott's and Greave's (VRH) model fits are tabulated in Table 3. It is notable that N(E_F) values from Mott's VRH fit are in the range of 10^{23} eV^{-1} cm^{-3}, whereas from the GVRH model fit, N(E_F) values are in the order of 10^{29} eV^{-1}

m^{-3}. The regression coefficients obtained for Mott's VRH fits are better than those for GVRH fits. Therefore, the MVRH model can be considered suitable for explaining conductivity behavior at low temperatures. The $N(E_F)$ values from the MVRH model are comparable to those of MoO_3–SeO_2–ZnO glasses[19] and CdO–V_2O_5–ZnO glasses[20].

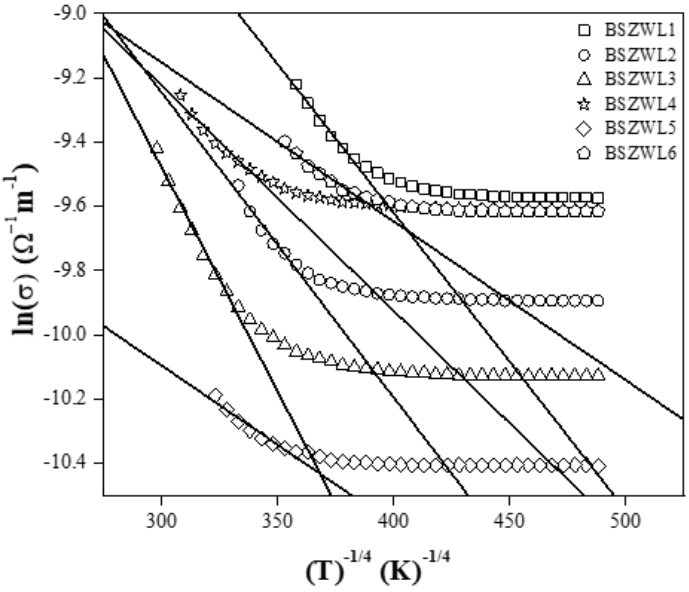

Fig 5. Mott's VRH plots of $\ln(\sigma)$ versus $T^{-1/4}$ for all BSZWL glasses

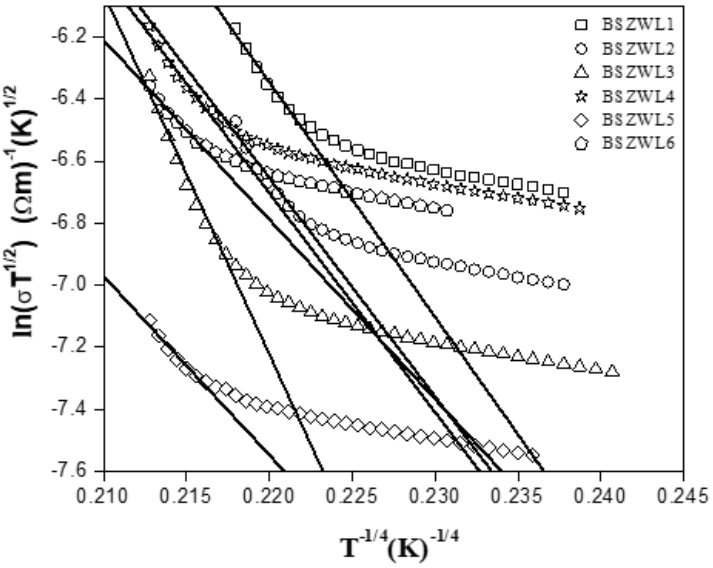

Fig 6. Greave's plots of $\ln(\sigma T^{1/2})$ versus $T^{-1/4}$ for all BSZWL glasses

4 Conclusion

A unit set of supposedly mechanically and thermally stable borosilicate glass nanocomposites in the composition, $xLi_2O + 0.15SiO_2 + 0.45B_2O_3 + 0.05ZnO + (0.35 - x)WO_3$: (Where x = 0.25, 0.26, 0.28, 0.30, 0.33, 0.34) have been synthesized.

- The samples are found transparent, stable and bubble free.
- The XRD spectra revealed nano-crystalline glassy phase of the samples. Crystallite sizes arefound to be the fraction of a nano meter.
- Density decreased from 2.9003 gm/cc to 2.4954 gm/cc and molar volume increase from 38.680 cm^3/mol to 44.569 cm^3/mol with increase in Li_2O.
- Glasses behaved like semiconductors in terms of conductivity variation with temperature. Conductivity varied in the range 10^{-4} $(\Omega m)^{-1}$ - 10^{-5} $(\Omega m)^{-1}$ within temperature range of interest. It decreased decrease with increase in Li_2O mole fractions up to 0.33 and increased for higher mole fractions.
- Conductivity behaviour, for temperature above $\Theta_D/2$, is found to be consistent with Mott's SPH model. Activation energy derived from SPH model fits is in the range 0.282 eV - 0.702 eV and was found to decrease with increase in Li_2O mole fractions up to 0.33 and increased for higher mole fractions.
- Decrease of conductivity and activation energy with Li_2O mole fractions has been attributed to dynamic nature of network and the formation of cation-polaron neutral entities.
- Low temperature conductivity, for below $\Theta_D/2$, is found to vary in accordance with Mott's VRH model and, the density of states at Fermi level derived from this model fits are of the order of 10^{23} $eV^{-1}cm^{-3}$ which agree with literature.

References

1) Nieves CA, Lanagan MT. Exploring the dielectric polarization and ionic conduction mechanisms in sodium-containing silicate and borosilicate glasses. *Journal of Non-Crystalline Solids*. 2023;617:122505. Available from: https://dx.doi.org/10.1016/j.jnoncrysol.2023.122505.
2) Alatawi AS, Alturki AM, Soliman GM, Abulyazied DE, Taha MA, Youness RA. Improved toughness, electrical conductivity and optical properties of bioactive borosilicate glasses for orthopedic applications. *Applied Physics A*. 2021;127(12). Available from: https://dx.doi.org/10.1007/s00339-021-05116-1.
3) El-Damrawi G, Abdelghany AM, Hassan AK, Faroun B. Effect of BO4 and FeO4 Structural Units on Conduction Mechanism of Iron Borosilicate Glasses. *Silicon*. 2021;13(11):4025–4031. Available from: https://dx.doi.org/10.1007/s12633-020-00694-w.
4) El-Damrawi G, Abdelghany AM, Hassan AK, Faroun B. Conductivity and morphological studies on iron borosilicate glasses. *Journal of Non-Crystalline Solids*. 2020;545. Available from: https://dx.doi.org/10.1016/j.jnoncrysol.2020.120233.
5) Malge A, Sankarappa T, Devidas GB, Sujatha T. Dielectric relaxation in zinc-borotellurite glasses doped with alkali, transition and rare earth oxides. In: Second International Conference on Applied Physics, Power and Material Science;vol. 1451 of Journal of Physics: Conference Series. IOP Publishing. 2020;p. 1–6. Available from: https://dx.doi.org/10.1088/1742-6596/1451/1/012014.
6) Taha TA, Alomairy S, Saad SA, Tekin HO, Al-Buriahi MS. Synthesis and dielectric relaxation behavior of 55B2O3–15SiO2– 30Na2O: WO3 glass system. *Ceramics International*. 2021;47(14):20201–20209. Available from: https://dx.doi.org/10.1016/j.ceramint.2021.04.027.
7) Moustafa MG, Shreif A, Ghalab S. Towards superior optical and dielectric properties of borosilicate glasses containing tungsten and vanadium ions. *Materials Chemistry and Physics*. 2020;254:123464. Available from: https://dx.doi.org/10.1016/j.matchemphys.2020.123464.
8) Abdel-karim AM, Fayad AM, El-kashef IM, Saleh HA. Influence of Vanadium Oxide on the Optical and Electrical Properties of Li (Oxide or Fluoride) Borate Glasses. *Journal of Electronic Materials*. 2023;52(4):2409–2420. Available from: https://dx.doi.org/10.1007/s11664-022-10187-8.
9) Ke Z, Cao X, Shan C, Shi L, Wang P, Yang Y, et al. The effect of alkali metal oxide on the properties of borosilicate fireproof glass: Structure, thermal properties, viscosity, chemical stability. *Ceramics International*. 2021;47(14):19605–19613. Available from: https://dx.doi.org/10.1016/j.ceramint.2021.03.298.
10) Kiey SAA, Abdel-Hameed SAM, Marzouk MA. Influence of Transition Metals on the Development of Semiconducting and Low Thermal Expansion TiO2-Borosilicate Glasses and Glass Ceramics. *Silicon*. 2024;p. 1–9. Available from: https://dx.doi.org/10.1007/s12633-024-02896-y.
11) Taha EO, Saeed A. The effect of cobalt/copper ions on the structural, thermal, optical, and emission properties of erbium zinc lead borate glasses. *Scientific Reports*. 2023;13(1):1–13. Available from: https://dx.doi.org/10.1038/s41598-023-39256-6.
12) Husenkhan DB, , Sankarappa T, Malge A. DC Conductivity of Lithium-Zinc-Boro- Phosphate Glasses. *Indian Journal of Science and Technology*. 2021;14(46):3416–3424. Available from: https://dx.doi.org/10.17485/ijst/v14i46.1890.
13) Ganvir VY, Ganvir HV, Gedam RS. Effect of Dy2O3 on Electrical Conductivity, Dielectric Properties and Physical Properties in Lithium Borosilicate Glasses. *Integrated Ferroelectrics*. 2019;203(1):1–11. Available from: https://dx.doi.org/10.1080/10584587.2019.1674947.
14) Gundale SS, Behare VV, Deshpande AV. Study of electrical conductivity of Li2O-B2O3-SiO2-Li2SO4 glasses and glass-ceramics. *Solid State Ionics*. 2016;298:57–62. Available from: https://dx.doi.org/10.1016/j.ssi.2016.11.002.
15) Moustafa MG, Morshidy H, Mohamed AR, El-Okr MM. A comprehensive identification of optical transitions of cobalt ions in lithium borosilicate glasses. *Journal of Non-Crystalline Solids*. 2019;517:9–16. Available from: https://dx.doi.org/10.1016/j.jnoncrysol.2019.04.037.
16) Devidas A, Sankarappa T, Malge A, Heerasingh M, Raghavendra B. Electrical and gamma ray shielding characteristics of zinc-borovanadate glasses mixed with MnO. *Journal of the Australian Ceramic Society*. 2023;59(2):391–402. Available from: https://dx.doi.org/10.1007/s41779-023-00840-8.
17) Devidas A, Sankarappa T, Malge A, Heerasingh M. Gamma-ray Shielding Characteristics and Electrical Properties of Na2O Doped Zinc-Boro-Vanadate Glasses. *Journal Transactions of the Indian Ceramic Society*. 2023;82(2):97–104. Available from: http://dx.doi.org/10.1080/0371750X.2023.2175040.
18) Ashwajeet JS, Sankarappa T, Sujatha T, Ramanna R. Thermal and electrical properties of (B2O3-TeO2-Li2O-CoO) glasses. *Journal of Non-Crystalline Solids*. 2018;486:52–57. Available from: https://dx.doi.org/10.1016/j.jnoncrysol.2018.02.010.

19) Biswas D, Ningthemcha RKN, Das AS, Singh LS. Structural characterization and electrical conductivity analysis of MoO3–SeO2–ZnO semiconducting glass nanocomposites. *Journal of Non-Crystalline Solids*. 2019;515:21–33. Available from: https://dx.doi.org/10.1016/j.jnoncrysol.2019.04.002.
20) Das AS, Roy M, Roy D, Bhattacharya S. DC electrical properties and non–adiabatic small polaron hopping in V2O5–CdO–ZnO glass nanocomposites. *Indian Journal of Pure & Applied Physics*. 2019;57(11):803–811. Available from: http://nopr.niscpr.res.in/handle/123456789/51724.